

Cite this: *J. Anal. At. Spectrom.*, 2012, **27**, 2123www.rsc.org/jaas

TECHNICAL NOTE

Optimizing sample and spike concentrations for isotopic analysis by double-spike ICPMS†

Seth G. John*

Received 20th July 2012, Accepted 20th September 2012

DOI: 10.1039/c2ja30215b

Double spike techniques are widely used for measuring the isotopic composition of natural samples. In order to achieve the most accurate results by double spike analysis, it is important to choose an appropriate double-spike composition, analyte concentration, and spike to natural ratio ($C_{\text{spk}}/C_{\text{nat}}$) where C_{nat} is the concentration of a sample or standard with a natural abundance of the isotopes and C_{spk} is the concentration of an added spike with an unnatural isotope composition. Here, the effect of varying these parameters is explored using a Monte Carlo technique which simulates error from counting statistics, Johnson noise, and isobaric interferences. Typically, optimal spike composition and $C_{\text{spk}}/C_{\text{nat}}$ are calculated under the constraint that total concentration of spike plus sample ($C_{\text{spk}} + C_{\text{nat}}$) must remain constant, so that as the amount of double spike is increased, the amount of sample is decreased. In practice, there is no reason for $C_{\text{spk}} + C_{\text{nat}}$ to be held constant, because an analyst with a fixed quantity of sample may add any amount of spike to this sample as long as detector limits are not exceeded. Therefore, here, double spikes are here optimized while allowing C_{spk} and C_{nat} to vary independently. For thirty three different elements, this new approach of allowing C_{spk} and C_{nat} to vary independently led to a decrease in theoretical error of up to ~30% in the absence of isobaric interferences. In the presence of isobaric interferences, this approach can deliver even larger improvements in accuracy and precision. Theoretical error is then compared to observed error both for $\delta^{56}\text{Fe}$ standards and for $\delta^{56}\text{Fe}$, $\delta^{66}\text{Zn}$, and $\delta^{114}\text{Cd}$ measured in seawater. Theoretical error and measured error for real seawater samples are highly correlated, with 78%, 85%, and 96% of observed error in $\delta^{56}\text{Fe}$, $\delta^{66}\text{Zn}$, and $\delta^{114}\text{Cd}$, respectively, accounted for using an error model which includes only Johnson noise and counting statistics. This confirms that such models, which minimize theoretical error, can be used to optimize spike composition, C_{spk} , and C_{nat} in order to increase accuracy and precision for analysis of natural samples.

1. Introduction

Double-spiking is a common method used to measure stable isotope ratios in natural samples. It may be used when an element has four or more stable isotopes, and relies on mixing together a sample, with an isotope ratio close to the natural abundance, with a “spike” made from highly purified isotopes which has an isotopic ratio very different from natural.¹ Analysis of the four isotopes in the spike–sample mixture by multi-collector mass spectrometry yields a highly accurate measurement of three independent isotope ratios. These three ratios are used to solve three unknown quantities: (1) the exact ratio of the concentration of spike to the concentration of sample ($C_{\text{spk}}/C_{\text{nat}}$), (2) amount of isotopic fractionation due to instrumental and/or methodological mass bias and (3) isotopic fractionation of the sample

compared to a standard. The use of a double-spike has several advantages over alternative methods for determining sample isotope ratios such as sample–standard bracketing.² For example, the double spike automatically corrects for any isotopic fractionation that occurs during sample processing (assuming the spike is added prior to processing), it can correct for differences in instrumental mass bias in samples compared to standards (e.g. due to sample matrix), and it can be used to yield a highly accurate measurement of sample concentration as long as the amount of double spike added is well known.

Analytical error in multi-collector ICP-MS can be described as the combination of several separate sources of error e.g. ref. 3. For low analyte signals (<~50 mV) the error is dominated by “Johnson noise” on the Faraday collectors. For larger signals (>~50 mV) the error is dominated by counting statistics. When large quantities of sample (>~2 V) are analyzed without a double spike, the error is dominated by a third process which has been hypothesized to be short-timescale ‘flicker’ in instrumental mass bias.³ When taken together, the entire variance observed during the analysis of a single

University of South Carolina, Department of Earth and Ocean Sciences, Columbia, SC, 29208, USA. E-mail: sjohn@geol.sc.edu

† Electronic supplementary information (ESI) available. See DOI: 10.1039/c2ja30215b

sample can be accounted for by these three processes.³ Johnson noise error is independent of the total signal strength (V) while counting statistics error is proportional to the square root of signal strength (\sqrt{V}). ‘Flicker’ error is hypothesized to be independent of signal strength, however it only becomes a major source of error at very high analyte concentrations greater than are measured by a typical mass spectrometer detector. Thus, under typical conditions, increased signal strength leads to decreased analytical error.

Because of the complexity of solving the double-spike calculations, the error associated with each of the four individual isotopes used in the double-spike calculations has a complex relationship to the error in the calculated sample isotopic composition. A variety of different techniques have been applied to find optimal values for the spike composition and spike to sample ratio ($C_{\text{spk}}/C_{\text{nat}}$) for double spike analyses. For example, a Monte Carlo simulation provides a simple approach to estimating the total error associated with different double spikes.⁴ Error can also be calculated linearly.^{5–7} Each of these techniques takes a slightly different approach to specifying errors. Johnson and Beard⁶ and Fantle and Bullen⁴ assume that the errors on any measured ratio are constant, regardless of signal strength. Galer⁵ calculates optimal $C_{\text{spk}}/C_{\text{nat}}$ and spike composition assuming that the error is only due to counting statistics and that total $C_{\text{spk}} + C_{\text{nat}}$ remains constant. Rudge *et al.*⁷ have developed a Matlab “double spike toolbox” that allows the user flexibility in specifying the error model used and the relationship between C_{spk} and C_{nat} . By default, the error model includes both counting statistics and Johnson noise and assumes a 10 V mean voltage for all measured isotopes, thus also keeping $C_{\text{spk}} + C_{\text{nat}}$ constant.

Previous techniques to predict error for different double-spike compositions and $C_{\text{spk}}/C_{\text{nat}}$ provide a valuable tool for future researchers seeking to develop a double-spike appropriate to their application. For example, the double-spike toolbox⁷ is publicly available and has already been used to predict optimal spike composition and $C_{\text{spk}}/C_{\text{nat}}$ for analysis of $\delta^{56}\text{Fe}$,⁸ $\delta^{66}\text{Zn}$,⁹ $\varepsilon^{114}\text{Cd}$,^{10,11} and $\delta^{44/42}\text{Ca}$.¹² Whenever the double-spike toolbox has been applied, the double-spike toolbox default assumption of constant $C_{\text{spk}} + C_{\text{nat}}$ has been used. Monte Carlo techniques are also used to predict optimal $C_{\text{spk}}/C_{\text{nat}}$, for example for $\delta^{56}\text{Fe}^{13}$ and $\delta^{53}\text{Cr}$,¹⁴ and an assumption of constant $C_{\text{spk}} + C_{\text{nat}}$ is also generally used for Monte Carlo methods.

Here, the common assumption of constant $C_{\text{spk}} + C_{\text{nat}}$ is reexamined, and the relationship between theoretical error and observed error is determined for $\delta^{56}\text{Fe}$, $\delta^{66}\text{Zn}$, and $\delta^{114}\text{Cd}$. The common practice of calculating ideal $C_{\text{spk}}/C_{\text{nat}}$ while assuming constant $C_{\text{spk}} + C_{\text{nat}}$ is reexamined because, in practice, it is possible to add more spike to any given sample without decreasing the amount of sample analyzed (*i.e.* C_{spk} and C_{nat} may be varied independently). Particularly in cases where sample quantity is limited, it may therefore be advantageous to optimize the predicted error assuming the entire sample is analyzed (constant C_{nat}) with varying amounts of spike, because of the relationship between error and signal strength. Of course, theoretical predictions for minimizing error are only useful to the extent that such techniques lead to a decreased error when analyzing actual samples. Therefore, theoretically predicted errors and observed errors are compared for $\delta^{56}\text{Fe}$ standards prepared at a wide variety of concentrations and $C_{\text{spk}}/C_{\text{nat}}$, and for 48 seawater dissolved-phase $\delta^{56}\text{Fe}$, $\delta^{66}\text{Zn}$, and $\delta^{114}\text{Cd}$ measurements.

2. Methods

2.1 Monte Carlo prediction of error

A Monte Carlo method is used to estimate the error associated with different spike compositions and spike to sample ratios. Four different possible sources of stochastic error are explored, and one process which causes systematic errors. Sources of stochastic error include (1) Johnson noise associated with the detector, also known as ‘Johnson–Nyquist noise’ or ‘thermal noise’ (2) counting statistics, also known as ‘shot noise’ (3) elemental isobaric interferences which can be corrected by measuring a different isotope of the interfering element (4) isobaric interferences, such as polyatomic species, which cannot be corrected for by measuring another mass. In addition, we examine the systematic offsets produced by an uncorrected isobaric interference. Based on these different sources of error, it is possible to calculate a single value of the total error associated with each of the four isotopes used in the double-spike calculation.

The four sources of stochastic error can be separately calculated for each isotope based on signal intensity. Johnson noise is assumed to be 18 μV for each 4.2 s integration period³ which is very similar to the 10 μV noise for an 8 s integration used by Rudge *et al.*⁷ The absolute error due to Johnson noise is:

$$\sigma_{\text{Johnson noise}}(V) = 3.69 \times 10^{-5} / \sqrt{\Delta t} \quad (1)$$

where t is the time in seconds. Counting statistics error is given by \sqrt{n} , where n is the total number of ions measured. Applying a conversion of $6.25 \times 10^7 \text{ cps V}^{-1}$ (applicable to the commonly used $10^{11} \Omega$ Faraday cup amplifier), the absolute error due to counting statistics is:

$$\sigma_{\text{counting statistics}}(V) = 1.265 \times 10^{-4} \sqrt{V/\Delta t} \quad (2)$$

When correcting for an elemental isobaric interference (*e.g.* using ^{60}Ni as a correcting isotope to calculate the magnitude of ^{58}Ni at mass 58, when using ^{58}Fe as part of a double-spike calculation), the error is:

$$\sigma_{\text{isobar correction}}(V) = \sqrt{(1.36 \times 10^{-9} + 1.60 \times 10^{-8} V)/\Delta t} \times f \quad (3)$$

where V is the signal intensity for the correcting isotope and f is correction factor equivalent to signal intensity ratio of the corrected isotope (*e.g.* ^{58}Ni) compared to the correcting isotope (*e.g.* ^{60}Ni). Finally, there may be a source of stochastic error due to the presence of an isobaric interference for which no correction is available, such as polyatomic interferences or single-element interferences. The magnitude of this error will depend on the nature of the interference, for example the variability in intensity for an elemental interference is generally much smaller than the variability in intensity for a polyatomic interference. This source of error is termed σ_{isobar} , and its magnitude must be determined experimentally. The total stochastic error associated with each of the individual isotopes ($\sigma_{\text{single isotope}}$) measured is therefore:

$$\sigma_{\text{single isotope}}^2 = \sigma_{\text{Johnson noise}}^2 + \sigma_{\text{counting statistics}}^2 + \sigma_{\text{isobar correction}}^2 + \sigma_{\text{isobar}}^2. \quad (4)$$

In addition to stochastic error, every isobaric interference is associated with an average voltage (V_{isobar}) which may lead to systematic inaccuracies in the measured voltage. If the isobaric interference can be corrected using another isotope of the same element, or if the magnitude of the isobar is equal in blanks and samples and the blank value can be subtracted from both, then $V_{\text{isobar}} = 0$. If this cannot be done, for example if the isobaric interference is more intense in samples compared to standards, the measured voltage will be the sum of spike voltage, sample voltage, and V_{isobar} , leading to systematic inaccuracies in the isotope ratio measured by double-spike analysis.

The error for each single isotope is propagated through the double spike equation by Monte Carlo simulation. First, average voltages for each isotope are determined based on the isotopic composition of spike–sample mixture and instrumental sensitivity. These voltages are then modified according to the predicted error for each single isotope to simulate multiple analyses of the same sample. Random numbers are generated using the Box–Muller transformation:

$$R_{\text{norm}} = \sqrt{-2 \ln R_1} \cos(2\pi R_2) / 0.707 \quad (5)$$

where R_1 and R_2 are pseudo-random numbers uniformly distributed between 0 and 1 generated using the Excel RAND() function, and R_{norm} is a population of normally distributed pseudo-random numbers with a standard deviation of 1. A random population of voltages for each isotope is calculated by multiplying $\sigma_{\text{single isotope}}$ by a unique value of R_{norm} , and adding this simulated error to the original voltage. If applicable, V_{isobar} is also added to this voltage. These voltages are used to calculate the sample isotopic composition for each simulated analysis according to the procedure outlined by Siebert *et al.*¹⁵ Five thousand simulated analyses are used to determine the standard deviation associated with any particular combination of sample and spike.

This technique has been implemented in an Excel spreadsheet (see ESI appendix†). Implementation in Excel has disadvantages, including the fact that Excel is computationally slower than alternatives (e.g. Matlab), and that the user-interface is relatively cumbersome for an experienced user compared to a command-line interface (e.g. Matlab). Particularly if a great number of hypothetical double-spikes are to be tested, it may be more efficient to modify the Matlab double-spike toolbox⁷ to take into account the additional sources of error discussed here, and to allow C_{spk} and C_{nat} to vary independently. Nonetheless, a Monte Carlo approach implemented in Excel is probably sufficient for an analyst exploring a small number of double spikes; Excel can calculate the error associated with 5000 different analyses in a fraction of a second and it is accessible to a large community of users.

2.2 Stable isotope ratio measurements

All isotopic analyses were performed at the University of South Carolina using a Neptune multi-collector ICP-MS (Thermo Scientific) with an Apex-Q desolvating sample introduction system (ESI). Samples were mixed with a double-spike prior to analysis and analyzed for 40 cycles over 168 s. Stable isotope ratios were calculated for each cycle using the data reduction scheme of Siebert *et al.*¹⁵ The stable isotope ratio value ($\delta^{56}\text{Fe}$,

$\delta^{66}\text{Zn}$, or $\delta^{114}\text{Cd}$) for each analysis was determined as the average ratio over all 40 cycles, and the error for each analysis was calculated as the standard error for the 40 cycles.

$\delta^{56}\text{Fe}$ was measured using a double-spike containing 0.003% ^{54}Fe , 0.7% ^{56}Fe , 47.7% ^{57}Fe and 51.6% ^{58}Fe . Samples were analyzed in high-resolution mode to exclude interferences such as ArN^+ , ArO^+ , and ArOH^+ . ^{53}Cr and ^{60}Ni were monitored to correct for interferences on ^{54}Fe and ^{58}Fe , respectively. $\delta^{66}\text{Zn}$ was measured using a double-spike containing 80% ^{64}Zn , 0.9% ^{66}Zn , 18.4% ^{67}Zn , and 1.0% ^{68}Zn . Samples were analyzed in high-resolution mode to exclude interferences such as ArSi^+ . ^{60}Ni was monitored to correct for a Ni interference on ^{64}Zn . $\delta^{114}\text{Cd}$ was measured using a double-spike containing 33.4% ^{110}Cd , 64.8% ^{111}Cd , 1.4% ^{112}Cd , and 0.4% ^{114}Cd . Samples were analyzed in low-resolution mode. ^{105}Pd was monitored to correct for a ^{110}Pd interference on ^{110}Cd , and ^{117}Sn was monitored to correct for Sn interferences on ^{112}Cd and ^{114}Cd .

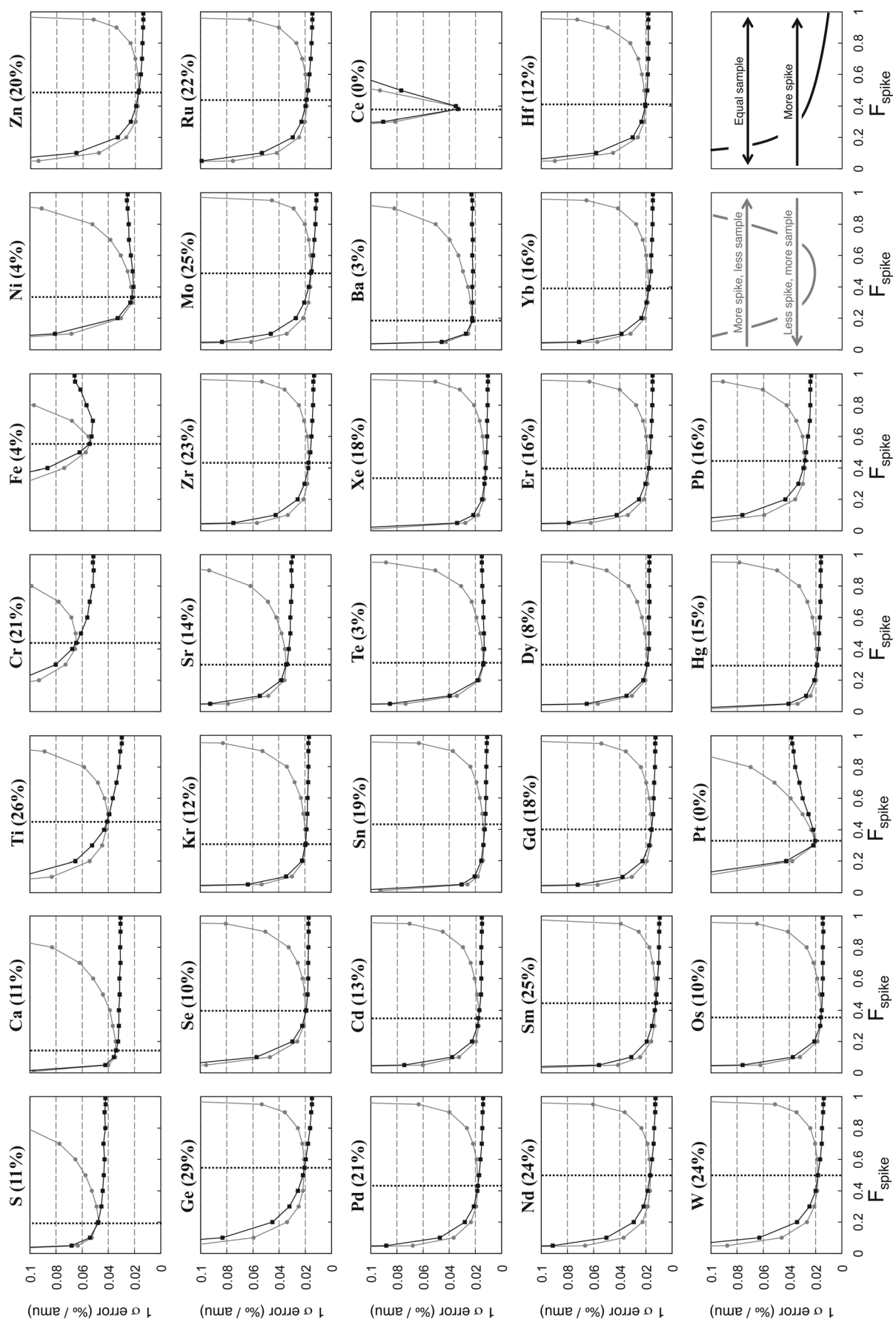
Seawater samples were collected in the eastern North Atlantic as part of the US GEOTRACES North Atlantic Zonal Transect. Fe, Zn and Cd were extracted onto Nobias resin at pH 6, and purified by anion exchange chromatography on AG-MP1 resin (manuscript in prep.). This method has high extraction efficiencies (>80% for all three metals) and purifies samples of relevant contaminants including major cations, Ni, Pd, Sn, and Mo.

3 Results and discussion

3.1 Predicting optimal $C_{\text{spk}}/C_{\text{nat}}$

3.1.1 Optimal $C_{\text{spk}}/C_{\text{nat}}$ without isobaric interferences. Using the Monte Carlo technique described above, errors have been predicted for 8s measurements of stable isotope ratios using a wide variety of C_{spk} and C_{nat} , where counting statistics and Johnson noise are the only sources of error. For the thirty-three isotope systems amenable to double-spike analysis, analytical error is predicted by Monte Carlo simulation as a function of proportion of spike in the spike–sample mixture (F_{spike}) (Fig. 1). Spike composition is based on the optimal theoretical spike composition for pure spikes predicted by Rudge *et al.*⁷ F_{spike} is calculated in two different ways. First, the double-spike toolbox default assumption of constant $C_{\text{spk}} + C_{\text{nat}} = 10$ V is used. Second, C_{nat} is held constant at the concentration corresponding to the optimal $C_{\text{spk}}/C_{\text{nat}}$ predicted by the double-spike toolbox, but C_{spk} is varied to achieve different values of F_{spike} .

In nearly all cases, predicted error is lower when C_{spk} and C_{nat} are allowed to vary independently, compared to constant $C_{\text{spk}} + C_{\text{nat}}$. Decreases in error range from 0% to 29% for the thirty-three isotope systems examined, with a mean improvement of 15%. The relationship between error and F_{spike} has a very different shape depending on whether C_{nat} or $C_{\text{spk}} + C_{\text{nat}}$ is held constant. With constant $C_{\text{spk}} + C_{\text{nat}}$, the error minimum is typically found for roughly equal amounts of sample and spike ($F_{\text{spike}} \approx 0.5$). With constant C_{nat} , error decreases monotonically as more spike is added (with the exceptions of Fe, Ce, and Pt), up to the maximum amount tested ($F_{\text{spike}} = 0.99$). Conceptually, the difference in these two curves can be explained by the exponential increase in error when either sample concentration or spike concentration becomes very low (Fig. 2). When $C_{\text{spk}} + C_{\text{nat}}$ is fixed, increasing C_{spk} leads to lower amounts of C_{nat} , with a



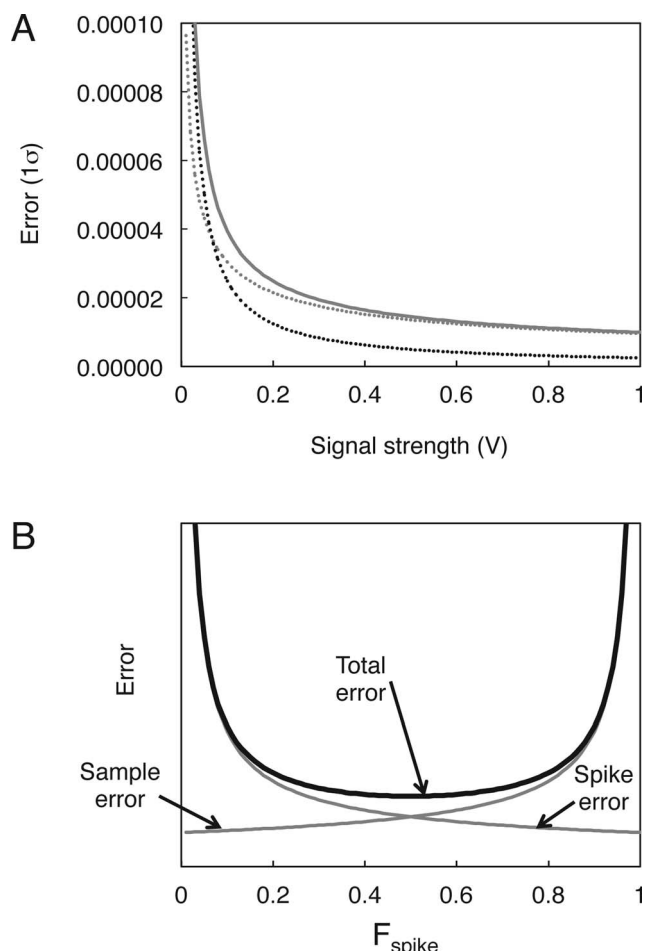


Fig. 2 The effect of sample and spike concentration on error. As the signal strength for any individual isotope decreases, there is an exponential increase in error due to Johnson noise (grey dashed line), counting statistics (black dashed line), and the combination of these two sources of error (solid grey line) (data pictured are for a 4 minute analysis with 10^{11} Ω resistors) (A). When $C_{\text{spk}} + C_{\text{nat}}$ is held constant, the total error depends in large part on separate errors for sample and spike. Therefore, total error increases at both high and low values of F_{spike} where either spike or sample concentration become very low (B).

consequent increase in error. When C_{nat} is fixed, increasing C_{spk} decreases error.

With fixed C_{nat} and variable C_{spk} , the predicted minimum error is typically found at the highest F_{spike} tested (0.99). Such high values of F_{spike} are unlikely to be useful in practice because they require a 100-fold excess of spike over sample. Thus, detector limits will be exceeded unless very small quantities of sample are used. However, the decrease in error is non-linear with increasing F_{spike} , so that most of the benefits of reduced error can be achieved by increasing F_{spike} by ~ 0.2 , compared to

the optimal spike concentration predicted for constant $C_{\text{spk}} + C_{\text{nat}}$, corresponding to a more reasonable doubling to tripling in spike concentration (Fig. 1).

Over a wide range of sample and spike concentrations, error predicted by Monte Carlo simulation matched the measured error for the analysis of $\delta^{56}\text{Fe}$ in standards (Fig. 3), suggesting that counting statistics and Johnson noise were the predominant sources of error. Techniques that minimize theoretically predicted error can therefore have a real impact on reducing error for analysis of $\delta^{56}\text{Fe}$ standards.

3.1.2 Optimal $C_{\text{spk}}/C_{\text{nat}}$ with isobaric interferences. If isobaric interferences are present on the isotopes used in the double spike, increasing C_{spk} with constant C_{nat} can greatly improve precision and decrease analytical error. Isobaric interferences can decrease data quality in two ways, uncorrected isobaric interferences decrease both accuracy and precision while corrected isobaric interferences decrease analytical precision only.

An uncorrected isobaric interference can cause inaccuracies in the calculated sample stable isotope ratio. These sorts of interferences occur, for example, when isobaric interferences are present only in samples, so that they cannot be corrected by on-peak zero using a blank. Using Monte Carlo simulation, inaccuracies have been predicted for adding 100 μV of a constant isobaric interference to each of the four Fe isotopes, while keeping C_{nat} constant (Fig. 4A). When the interference is added on ^{57}Fe or ^{58}Fe , the two isotopes in the double-spike, there is a monotonic decrease in inaccuracy at higher spike concentrations. The magnitude of this inaccuracy decreases in a roughly linear fashion as $\sqrt{C_{\text{spk}}}$ increases, so that increasing C_{spk} by a factor of four leads to halving the inaccuracy. The relationship between accuracy and C_{spk} is more complicated for interferences on ^{54}Fe and ^{56}Fe , accuracy decreases as F_{spike} decreases from 0 to ~ 0.1 , and slightly increases thereafter. The theoretically predicted relationship between accuracy and C_{spk} is matched by observations, when $\delta^{56}\text{Fe}$ is measured with an altered cup configuration which collects both Fe and interferences at mass 57 (potential interferences include ArOH^+) and mass 58 (potential interferences include ArOHH^+ and $^{57}\text{FeH}^+$) (Fig. 4B). In both cases, inaccuracy decreases in a roughly linear fashion as $\sqrt{C_{\text{spk}}}$ increases. Both theory and data therefore confirm that if uncorrected isobaric interferences are present on isotopes used in the double-spike, increasing C_{spk} increases accuracy.

Isobaric interferences also add stochastic error, or “noise”. All isobaric interferences contribute to noise, even if the average signal associated with each interference can be corrected by on-peak zero, or by monitoring another isotope of the interference to subtract the interference (e.g. monitoring ^{60}Ni in order to correct for ^{58}Ni when measuring Fe isotopes). Using Monte Carlo simulation, the effect of noise from an isobaric interference is predicted when adding 100 μV of noise to each of the four Fe

Fig. 1 For the 33 elements with four or more stable isotopes, error is predicted by Monte Carlo simulation, where F_{spike} is the fraction of spike in the spike-sample mixture and error is presented as the 1σ error for a single 8s measurement in permil per amu ($\text{‰}/\text{amu}$). Grey lines are based on the approach of Rudge *et al.*⁷ using their optimal spike composition and assuming constant $C_{\text{spk}} + C_{\text{nat}}$ of 10 V across all isotopes, with dashed black vertical lines drawn at the error minimum. Black lines are error predictions using the spike composition and sample concentration found to minimize error with constant $C_{\text{spk}} + C_{\text{nat}}$, but allowing for varying amounts of spike. Above each plot is the percentage decrease in error for constant C_{nat} and variable C_{spk} , compared to constant $C_{\text{spk}} + C_{\text{nat}}$.

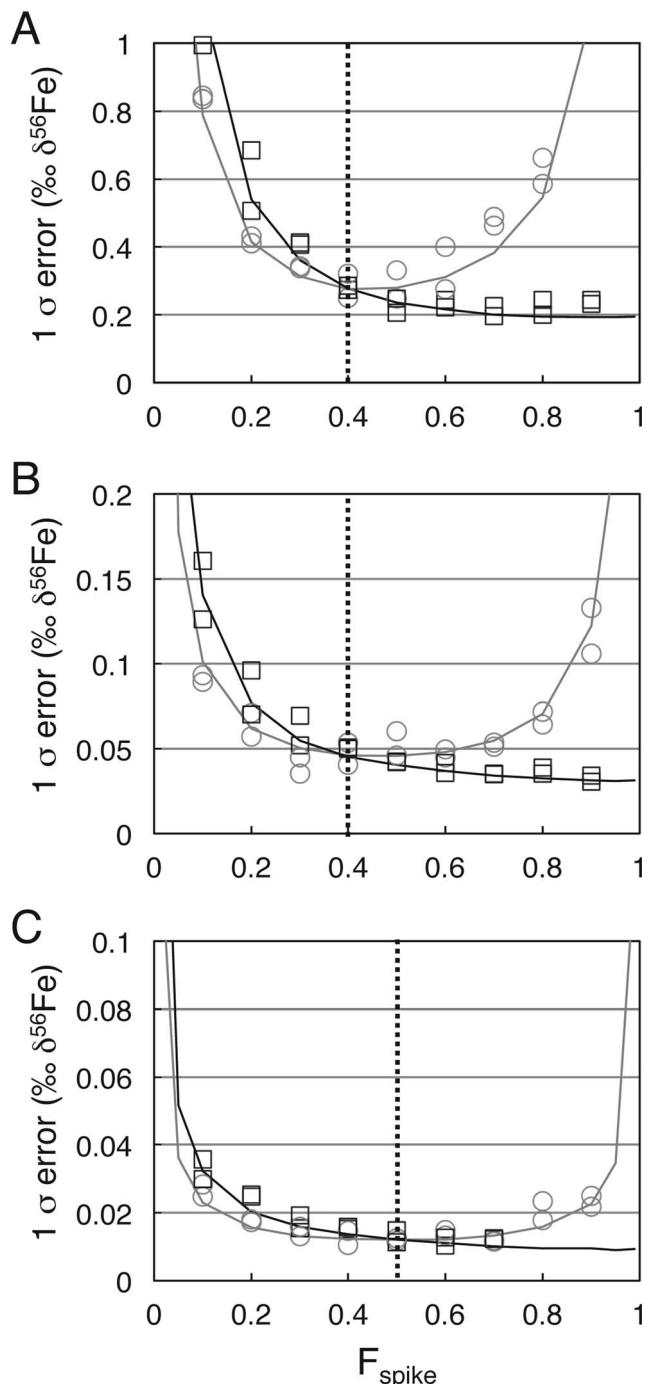


Fig. 3 Comparison of observed analytical error (open symbols) with error predicted by a Monte Carlo simulation (solid lines). Tests reflect a 4 minute analysis performed under an assumption of constant $C_{\text{spk}} + C_{\text{nat}}$ (grey lines and circles) and under an assumption of constant C_{nat} with variable C_{spk} (black lines and squares). Dashed black vertical lines are shown at the error minimum for constant $C_{\text{spk}} + C_{\text{nat}}$, and C_{nat} at this error minimum is used for the assumption of constant C_{nat} . Concentration ranges tested include 2 ppb $C_{\text{spk}} + C_{\text{nat}}$ versus fixed 1.2 ppb C_{nat} (A), 20 ppb $C_{\text{spk}} + C_{\text{nat}}$ versus fixed 12 ppb C_{nat} (B), and 200 ppb $C_{\text{spk}} + C_{\text{nat}}$ versus fixed 100 ppb C_{nat} (C).

isotopes (Fig. 5A). Similar to the effect on accuracy, increasing C_{spk} leads to a monotonic decrease in error when there is an interference on ^{57}Fe or ^{58}Fe . Error decreases in a roughly linear

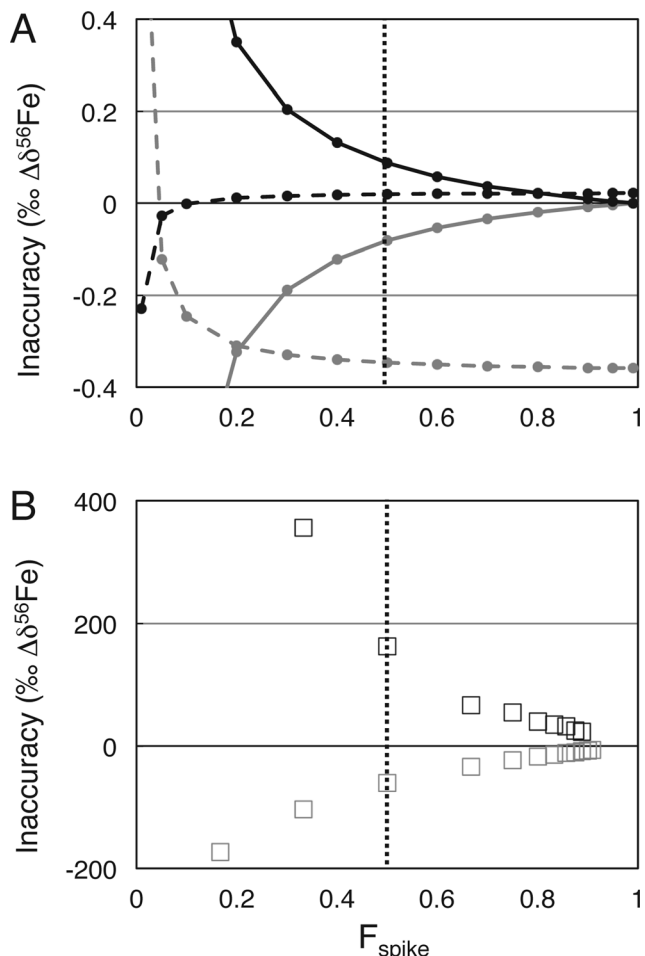


Fig. 4 The effect of isobaric interferences on analytical accuracy. Inaccuracy is predicted by Monte Carlo simulation for a 4 minute analysis with constant sample signal intensity (5 V) and variable spike. Simulations include the effect of 100 μV constant interference on ^{54}Fe (dashed grey line), ^{56}Fe (dashed black line), ^{57}Fe (solid black line), and ^{58}Fe (solid grey line), where $\Delta \delta^{56}\text{Fe}$ is the difference from the true standard $\delta^{56}\text{Fe}$ (A). The observed effect on analytical accuracy was measured by including isobaric interferences at mass 57 (black squares) and mass 58 (grey squares) after changing the cup configuration (B). Dashed black vertical lines are shown at the error minimum predicted for constant $C_{\text{spk}} + C_{\text{nat}}$.

fashion as $\sqrt{C_{\text{spk}}}$ increases, until C_{spk} is so high that the isobaric interference no longer dominates error. When noise is added to ^{56}Fe , there is also a monotonic decrease in error with increasing C_{spk} . When noise is added to ^{54}Fe , error decreases as F_{spike} increases from 0 to ~ 0.1 , and slightly increases thereafter. Observations when isobaric interferences are intentionally collected at mass 57 and 58 during analysis of $\delta^{56}\text{Fe}$ are similar to predictions (Fig. 5B). In both cases, error decreases dramatically as C_{spk} increases. Both theory and data therefore validate an approach of increasing C_{spk} in order to minimize error associated with isobaric interferences.

3.2 Predicted error and observed error for natural samples

Errors predicted by Monte Carlo simulation have been compared with measurements of natural samples. Seawater

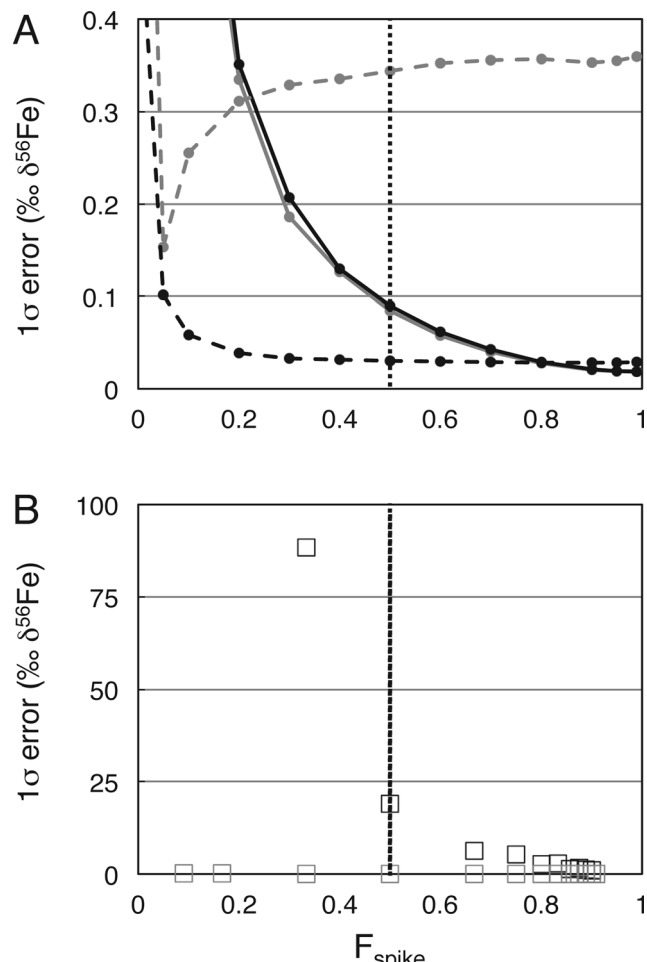


Fig. 5 The effect of isobaric interferences on analytical precision. Imprecision is predicted by Monte Carlo simulation for a 4 minute analysis with constant sample signal intensity (5 V) and variable spike. Shown is the simulated error with an extra 100 µV noise on ⁵⁴Fe (dashed grey line), ⁵⁶Fe (dashed black line), ⁵⁷Fe (solid black line), and ⁵⁸Fe (solid grey line) (A). The observed effect of polyatomic interferences is shown by altering the cup configuration so that both Fe and isobaric interferences are collected at mass 57 (black squares) and mass 58 (grey squares) (B). Observed errors including the isobaric interferences at mass 58 show a similar pattern to isobaric interferences at mass 57, though the magnitude of these interferences is much smaller. Dashed black vertical lines are shown at the error minimum for constant $C_{\text{spk}} + C_{\text{nat}}$.

samples were chosen for this comparison because seawater represents one of the most challenging matrices studied. Fe, Zn, and Cd are present in seawater at concentrations ranging from several nanomolar in deep waters to picomolar in surface waters. Meanwhile, a complex mixture of other salts is present in seawater at orders of magnitude higher concentrations than the analytes of interest. Comparing theoretical and observed errors for such challenging samples is therefore a good test of whether our model is correctly describing the most important sources of error which will be encountered for natural samples. For 48 samples of Fe, Zn and Cd extracted from seawater, observations of internal error, intermediate error, and external error are compared with errors predicted using Monte Carlo simulation.

Observed and predicted internal errors were highly correlated for analysis of seawater $\delta^{56}\text{Fe}$, $\delta^{66}\text{Zn}$, and $\delta^{114}\text{Cd}$ (Fig. 6A). The slopes of observed error plotted against predicted error were 0.97 for $\delta^{56}\text{Fe}$, 1.20 for $\delta^{66}\text{Zn}$, and 1.10 for $\delta^{114}\text{Cd}$ for best-fit lines forced through the intercept. These slopes suggest that our Monte Carlo method accurately predicts error for $\delta^{56}\text{Fe}$, and slightly under predicts error for $\delta^{66}\text{Zn}$ and $\delta^{114}\text{Cd}$. This under prediction might result from an error in the blank subtracted from each sample, an inaccuracy in the assumed spike and/or standard composition used in the double-spike calculation, or an uncorrected isobaric interference. Observed error seems to exceed predicted error in $\delta^{66}\text{Zn}$ and $\delta^{114}\text{Cd}$ more often when errors are large ($>0.2\text{\textperthousand}$), suggesting that special care should be taken when relating predicted and observed error for very small sample quantities.

Internal errors were also compared to “intermediate errors”, or the error between replicate analyses of a single sample during different analytical sessions or at different points during the same analytical session. Graphically, this can be observed by plotting the difference between two replicate analyses of $\delta^{56}\text{Fe}$, $\delta^{66}\text{Zn}$, or $\delta^{114}\text{Cd}$ against the predicted variance in this difference (based on the internal errors of the two separate measurements) (Fig. 6B). Statistically, this relationship is examined using the *t*-test. The 24 values of *t* had a standard deviation of 1.32 for $\delta^{56}\text{Fe}$, 0.98 for $\delta^{66}\text{Zn}$, and 0.95 for $\delta^{114}\text{Cd}$, suggesting that intermediate error for Cd and Zn were due entirely to internal error, but that ~25% of the intermediate error for Fe was due to some other source. A previous study on measurement of $\delta^{56}\text{Fe}$ in seawater found that internal error accounts for all of intermediate error in a sample-standard bracketing technique where a double-spike is not used, suggesting that this extra source of intermediate error is an isobaric interference at mass 57, 58, or 60. Finally, the relationship between internal error and true external error has been tested by doping four metal-free seawater samples with Fe, Zn, and Cd isotope standards, extracting and purifying these metals, and measuring $\delta^{56}\text{Fe}$, $\delta^{66}\text{Zn}$, and $\delta^{114}\text{Cd}$. In all cases, external error was similar to internal errors.

Overall, the error predicted theoretically by Monte Carlo simulation accounts for 78%, 85%, and 96% of the observed error for analysis of seawater $\delta^{56}\text{Fe}$, $\delta^{66}\text{Zn}$, and $\delta^{114}\text{Cd}$ by double-spike, respectively. This suggests that counting statistics and Johnson noise are the primary sources of error. Techniques which decrease error due to these sources, for example by increasing the amount of spike run with a fixed quantity of sample, are therefore expected to result in real-world benefits in terms of reduced error. If the unaccounted for error is due to uncorrected isobaric interferences, and if these errors occur at the same mass as the isotopes used in the double-spike, then increasing C_{spk} may also reduce this error.

3.3 Optimizing double-spikes when sample is not limited

Here, the discussion has focused primarily on minimizing error with fixed C_{nat} . This is particularly relevant when analyte concentrations are small, for example when analyzing trace metal isotopes in seawater. When sample is not limited, however, there are still benefits to optimizing spike composition and $C_{\text{spk}}/C_{\text{nat}}$ while allowing C_{spk} and C_{nat} to vary independently.

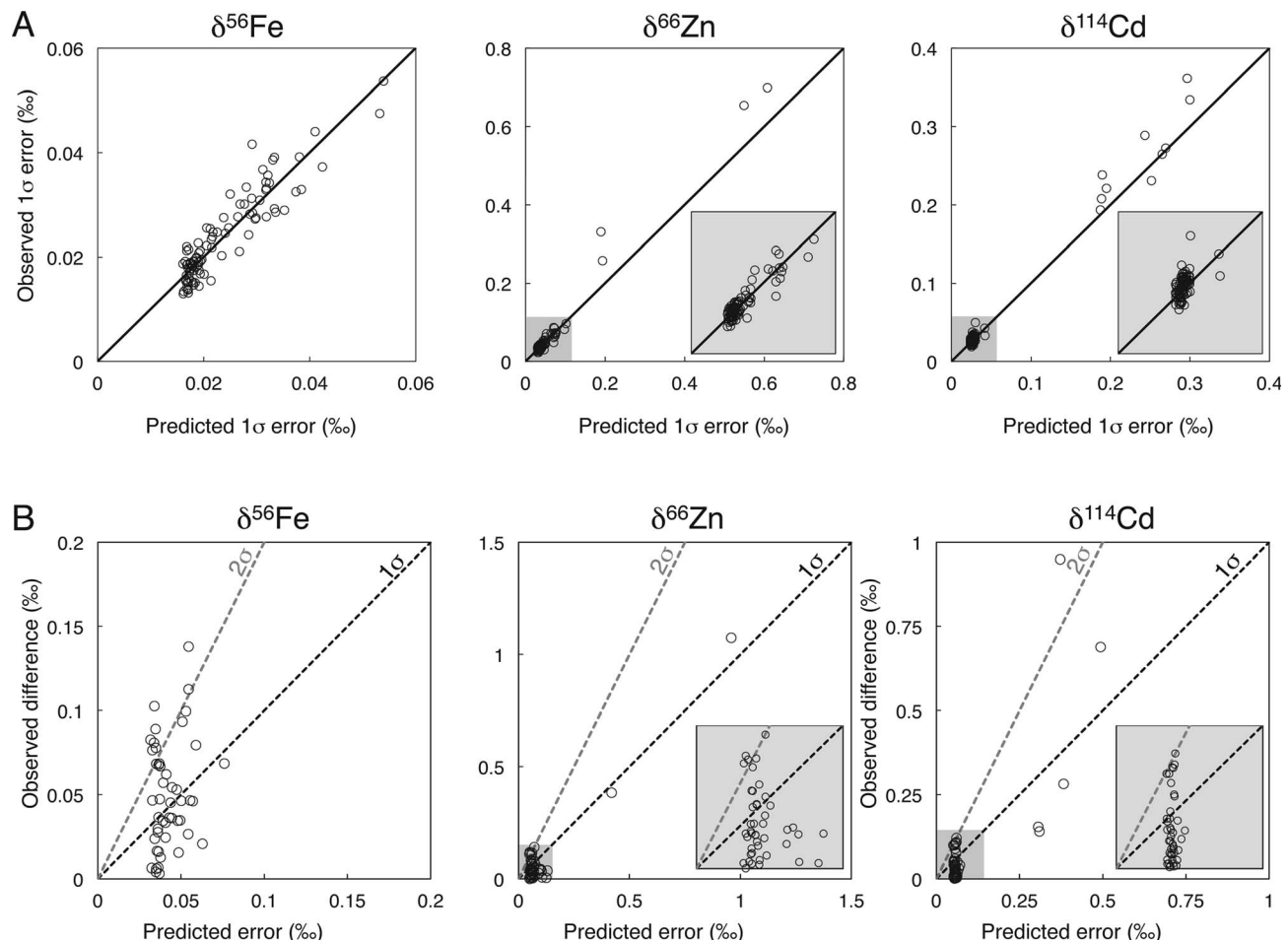


Fig. 6 Error predicted by Monte Carlo simulation compared to observed error for natural samples of Fe, Zn, and Cd extracted and purified from 48 one-liter seawater samples collected in the North Atlantic. Measured internal error is roughly proportional to the internal error predicted by Monte Carlo simulation (A). The observed difference between replicate measurements of the same sample are also correlated to predicted error (B). If observed differences were due entirely to theoretically predicted sources of error, ~68% of points should lie below the 1 σ line (black dashed line) and ~95% should lie below the 2 σ line (grey dashed line). Inset plots are a magnification of the grey-shaded region.

For example, Rudge *et al.*⁷ assume constant $C_{\text{spk}} + C_{\text{nat}}$ to find that the optimal spike for $\delta^{56}\text{Fe}$ is 77% ^{56}Fe and 23% ^{58}Fe with $F_{\text{spike}} = 0.55$. Because ^{56}Fe is already the dominant natural isotope (92%), however, using this spike limits the amount of sample that can be run without overloading the detectors. Assuming a limit of 50 V for any single detector, only 27 V of sample and 32 V of spike could be run under these conditions, leading to a total error in $\delta^{56}\text{Fe}$ of 0.008‰ over a 4 minute analysis. Error is 28% lower using a spike composed of 48% ^{57}Fe and 52% ^{58}Fe and $F_{\text{spike}} = 0.64$, because 54 V of sample and 96 V of spike can be analyzed without overloading any individual detector. Similarly, the use of a ^{64}Zn rich spike for Zn isotope analysis⁹ limits the total amount of sample that can be run, because ^{64}Zn is also the most naturally abundant isotope.

4. Conclusions

Observed analytical error in double-spike ICP-MS is well-predicted by a model including counting statistics and Johnson noise, confirming the value of theoretical approaches to minimizing error. While past work has focused on optimizing

$C_{\text{spk}}/C_{\text{nat}}$ assuming constant $C_{\text{spk}} + C_{\text{nat}}$ e.g. ref. 5 and 7, it is shown here that theoretical error can be reduced further when C_{spk} and C_{nat} are varied independently.

The Monte Carlo simulation provided here (ESI†) is a tool for choosing spike compositions and $C_{\text{spk}}/C_{\text{nat}}$ that are appropriate for a particular application. The following ‘rules of thumb’ are provided to help guide this process:

(1) Spike compositions predicted assuming constant $C_{\text{spk}} + C_{\text{nat}}$ are a good starting point for double-spike analysis. The error for badly composed spike can be orders of magnitude higher than for ‘optimal’ spike compositions e.g. ref. 5 and 7, while the error reductions for different C_{spk} and C_{nat} are generally smaller.

(2) There is no logical reason to use “optimal” $C_{\text{spk}}/C_{\text{nat}}$ ratios chosen based on an assumption of constant $C_{\text{spk}} + C_{\text{nat}}$. Instead, sample and spike concentrations should be chosen independently to minimize error.

(3) If sample is limited and isobaric interferences are not expected, error will often be reduced by adding as much spike as possible to your samples without exceeding detector limits. Note that there are typically diminishing returns for $C_{\text{spk}}/C_{\text{nat}}$ above

~ 3 (e.g. Fig. 2–5) so that it may be convenient to run all samples at the same $C_{\text{spk}}/C_{\text{nat}}$, regardless of the sample concentration.

(4) If sample is unlimited and isobaric interferences are not expected, consider mixing sample and spike in a such a way as to maximize signal on the least-abundant isotope.

(5) If isobaric interferences are expected, pay special attention to increasing sample or spike signal at this mass. When the isobaric interference is the major source of error, both inaccuracy and imprecision are expected to decrease roughly in proportion to increasing \sqrt{V} , where V is signal strength at the mass afflicted by the interference (e.g. Fig. 4 and 5).

References

- 1 M. H. Dodson, *J. Sci. Instrum.*, 1963, **40**, 289.
- 2 F. Albarède and B. Beard, in *Rev Mineral Geochem* 2004, vol. 55, p. 113.
- 3 S. G. John and J. F. Adkins, *Mar. Chem.*, 2010, **119**, 65.
- 4 M. S. Fantle and T. D. Bullen, *Chem. Geol.*, 2009, **258**, 50.
- 5 S. J. G. Galer, *Chem. Geol.*, 1999, **157**, 255.
- 6 C. M. Johnson and B. L. Beard, *Int. J. Mass Spectrom.*, 1999, **193**, 87.
- 7 J. F. Rudge, B. C. Reynolds and B. Bourdon, *Chem. Geol.*, 2009, **265**, 420.
- 8 M. A. Millet, J. A. Baker and C. E. Payne, *Chem. Geol.*, 2012, **304**, 18.
- 9 T. Arnold, M. Schonbachler, M. Rehkamper, S. F. Dong, F. J. Zhao, G. J. D. Kirk, B. J. Coles and D. J. Weiss, *Anal. Bioanal. Chem.*, 2010, **398**, 3115.
- 10 Z. C. Xue, M. Rehkamper, M. Schonbachler, P. J. Statham and B. J. Coles, *Anal. Bioanal. Chem.*, 2012, **402**, 883.
- 11 T. J. Horner, M. Schonbachler, M. Rehkamper, S. G. Nielsen, H. Williams, A. N. Halliday, Z. Xue and J. R. Hein, *Geochem. Geophys. Geosyst.*, 2010, **11**, DOI: 10.1029/2009gc002987.
- 12 R. S. Hindshaw, B. C. Reynolds, J. G. Wiederhold, R. Kretzschmar and B. Bourdon, *Geochim. Cosmochim. Acta*, 2011, **75**, 106.
- 13 F. Lacan, A. Radic, M. Labatut, C. Jeandel, F. Poitrasson, G. Sarthou, C. Pradoux, J. Chmeleff and R. Freydier, *Anal. Chem.*, 2010, **82**, 7103.
- 14 P. Bonnand, I. J. Parkinson, R. H. James, A. M. Karjalainen and M. A. Fehr, *J. Anal. At. Spectrom.*, 2011, **26**, 528.
- 15 C. Siebert, T. F. Nagler and J. D. Kramers, *Geochem., Geophys., Geosyst.*, 2001, **2**, DOI: 10.1029/2000GC000124.